Journal of Sound and Vibration (1999) **225**(2), 283–305
Article No. jsvi.1999.2270, available online at http://www.idealibrary.com on IDEAL®

APPROXIMATIONS OF THE DISPERSION RELATION FOR AN ELASTIC PLATE COMPOSED OF STRONGLY ANISOTROPIC ELASTIC MATERIAL

G. A. ROGERSON

Department of Computer and Mathematical Sciences, University of Salford, Salford, M5 4WT, England

AND

L. Y. KOSSOVITCH

Department of Mathematical Theory of Elasticity and Biomechanics, Saratov State University, Astrakhanskaya Srt. 83, *Saratov* 410601, *Russia*

(*Received* 15 *May* 1998, *and in final form* 8 *February* 1999)

In this paper approximations of the dispersion relation associated with harmonic waves propagating along the axis of transverse isotropy, parallel to the traction free surfaces, in a fibre-reinforced elastic plate are derived. High and low wave number expansions are derived which have potential applications to impact problems within plates and shells and acoustic scattering and radiation respectively. Plots of the associated group velocity curves are presented and a wave front travelling with a speed of the same order of magnitude as the Young's modulus along the fibre direction is observed. A particularly interesting feature of this front is that its formation arises through the cumulative effect of various harmonics in adjacent wave number regimes. The paper concludes with both a conjecture concerning the properties of this wave as the Young's modulus increases and the derivation of approximate solutions for the dispersion relation in the neighbourhood of the associated wave front.

1. INTRODUCTION

The use of fibre-reinforced composites is prevalent in modern structures. Such materials have found extensive use in the aerospace industry where their high strength-to-weight ratio is an integral part of aircraft design. Such composites are usually formed by reinforcing an elastic matrix with a series of strong parallel fibres. A typical composite consists of about a 60% volume fraction of carbon fibres embedded in a thermoplastic resin, with the fibre diameter and inter-fibre spacing of the order of 6 μm. In this paper such a material shall be treated as a homogeneous continuum. By treating the composite as such it is then tacitly assumed that the fibres are an inherent material property, rather than some form of inclusion. The specific problem studied in this paper is that of harmonic wave propagation along the direction of transverse isotropy, termed the fibre direction,

0022-460X/99/320283 + 23 $30.00/0

in a transversely isotropic elastic plate. In view of the aforementioned assumptions wave motion is then regarded, as with many earlier authors, e.g. [1, 2], as a phenomenon governed by the macroscopic properties of the material.

Theoretical and experimental investigation of wave propagation and vibration in fibre-reinforced structures is an area which has received a huge amount of interest in recent years owing to many industrial applications of such structures. A detailed list of references may be found in the review articles [3, 4]. Although most of the work in this area has been carried out within the framework of transversely isotropic elasticity, some related work has also been carried out for a more general orthotropic case [5–7]. In all this extensive literature it would seem that little consideration has been given to asymptotically approximating the dispersion relation and seeking to utilize such approximations in elucidation of wave and vibration phenomena. The primary purpose of this paper is to derive high and low wave number representations of the dispersion relation for a transversely isotropic elastic plate. It is expected that such approximations will help in the numerical inversion of the transform solutions often used to determine transient impact response [8]. Such methods, which involve the full three-dimensional equations of elasticity, are extremely important in the case of high-velocity impact response of fibre-reinforced composites, owing to the high stress gradients which may make various approximate theories inaccurate. Specifically, with this method exact transform solutions are obtained and numerical techniques are utilized only in the inversion of the integral transforms to recover dependence on space and time, this necessitating integration over an infinite wave number region and summation over all branches of the dispersion relation. For line impact problems it has previously been found that the denominator of the solution integrand is the associated dispersion relation [9]. In view of the fact that in practice the integral must be both restricted to a finite wave number range, and the summation of such integrals restricted to a finite number of branches, it is envisaged that the expansions derived in this paper will aid such inversion procedures.

In addition to the use of fibre-reinforced composites in the aerospace industry many cylindrical structures, such as pipes, are reinforced by fibres, often helically wound. Moreover in a recent paper [10] it has been shown that the asymptotic behaviour of the dispersion relation associated with an isotropic elastic thin cylinder is intimately related to that of an infinite elastic plate. So, in addition to applications to problems involving layered fibre-reinforced structures, it is envisaged that the present study, in which high wave number approximations of the dispersion relation for a fibre-reinforced plate are derived, will also provide results relevant to problems involving fibre-reinforced cylinders and cylindrical shells.

In section 2 the governing equations are derived and the dispersion relation is obtained. This relation is then decomposed into flexural and extensional components. In section 3 high wave number expansions for each harmonic of the dispersion relations associated with both flexural and extensional waves are derived. In section 4 similar expansions are derived appropriate for the low wave number region. Numerical results are presented in section 5 in which the high wave number approximations are shown to provide excellent agreement over a remarkably wide wave number range. It is also noted that the similar limit of the

fundamental modes yields the associated surface wave speed equation. It is further observed that a wave front is formed from the cumulative effect of the harmonics in adjacent wave number regions, this manifesting itself through the flattening of the dispersion curve branches at the appropriate wave speed. Group velocity curves are presented which confirm this and show a series of associated flat local maxima. Similar plots in respect of surface waves have been previously reported in reference [11] and a corresponding wave front observed in the numerical solution in reference [9]. In Section 6 the effect of increasing the Young's modulus in the fibre direction is discussed. It is shown that the wave front formed by the cumulative effect of the harmonics in adjacent wave number regions now has high speed. Moreover, the associated maxima on the group velocity curves occur for the first few harmonics are closely packed in the low wave number region. It is conjectured that as the associated wave has small amplitude and this amplitude tends to zero as the inextensible limit is reached. This section is concluded with the derivation of some approximate solutions for the dispersion relations in the neighbourhood of this wave front. Finally, in section 7 a discussion concerning the potential application of the approximate solutions is presented.

2. GOVERNING EQUATIONS FOR AN INFINITE PLATE

The concern in this paper is an infinite plate of width $2h$ composed of transversely isotropic elastic material. Attention will be restricted to the case of the direction of transverse isotropy laying in the plane of the plate, this being both mathematically expedient and common in engineering applications. A Cartesian co-ordinate system of axes $Ox_1x_2x_3$ is chosen with origin O in the mid-plane, Ox_3 normal of the plate and Ox_1 coincident with the direction of transverse isotropy. The equations of motion are assumed in their usual form:

$$\sigma_{ij,j} = \rho \ddot{u}_i, \tag{2.1}$$

in which ρ is the material density, $\sigma_{ij}(\mathbf{x}, t)$ the components of the Cauchy stresss tensor, and $u_i(\mathbf{x}, t)$ the components of displacement for a particle at position $\mathbf{x}$ at time t. Throughout this paper the summation convention on repeated suffices is understood, a superimposed dot indicates differentiation with respect to time and a comma differentiation with respect of the implied component of $\mathbf{x}$. Equations (2.1) are to be solved subject to traction-free boundary conditions on the upper and lower faces of the plate, namely

$$\sigma_{i3} = 0, \quad i = 1, 2, 3, \quad \text{at } x_3 = \pm h. \tag{2.2}$$

The stress–strain relationshsip for a transversely isotropic elastic material is well-known and may be expressed in the component form

$$\begin{aligned}\sigma_{ij} = {} & \lambda e_{kk}\delta_{ij} + 2\mu_T e_{ij} + \alpha(a_k a_m e_{km}\delta_{ij} + a_i a_j e_{kk}) \\ & + 2(\mu_L - \mu_T)(a_i a_k e_{kj} + a_j a_k e_{ki}) + \beta a_k a_m e_{km} a_i a_j.\end{aligned} \tag{2.3}$$

(see example reference [12]). In equation (2.3) $\mathbf{a}$ is a unit vector defining the axis of transverese isotropy and $\alpha, \beta, \lambda, \mu_T$ and μ_L are material constants. These material

constants may be related to the components of the symmetric stiffness matrix c_{pq}, commonly employed in crystal acoustics, through the expressions

$$c_{11} = \lambda + 2\mu_T = c_{22}. \qquad c_{33} = \lambda + 4\mu_L - 2\mu_T + 2\alpha + \beta,$$

$$c_{44} = \mu_L = c_{55}, \qquad c_{66} = \tfrac{1}{2}(c_{11} + c_{22}) = \mu_T,$$

$$c_{12} = \lambda, \qquad c_{13} = \lambda + \alpha = c_{23},$$

(see reference [13]). When the direction of transverse isotropy, referred to as the *fibre* direction, is along Ox_1 the components of stress are given explicitly through the relations

$$\sigma_{11} = (\lambda + 4\mu_L - 2\mu_T + 2\alpha + \beta)e_{11} + (\lambda + \alpha)(e_{22} + e_{33}), \tag{2.4}$$

$$\sigma_{22} = (\lambda + \alpha)e_{11} + (\lambda + 2\mu_T)e_{22} + \lambda e_{33}, \tag{2.5}$$

$$\sigma_{33} = (\lambda + \alpha)e_{11} + \lambda e_{22} + (\lambda + 2\mu_T)e_{33}, \tag{2.6}$$

$$\sigma_{12} = 2\mu_L e_{12}, \qquad \sigma_{13} = 2\mu_L e_{13}, \qquad \sigma_{23} = 2\mu_T e_{23}, \tag{2.7}$$

in which the infinitesimal strain tensor is defined in terms of the components of displacement through the relations

$$e_{ij} = \tfrac{1}{2}(u_{i,j} + u_{j,i}) \tag{2.8}$$

It is noted in passing that the limit of a material which is inextensible in the direction of transverse isotropy is examined by allowing $\beta \to \infty$, $e_{11} \to 0$, in such a way that $\beta e_{11} \to T$, an arbitrary tension along **a**. The typical situation addressed in this paper is strongly anisotropic media for which β is very much larger in magnitude than λ, μ_L, μ_T and α.

Utilization of equations (2.4)–(2.8) in the equations of motion (2.1) yields

$$c_5^2 \frac{\partial^2 u_1}{\partial x_1^2} + c_4^2\left(\frac{\partial^2 u_2}{\partial x_1 \partial x_2} + \frac{\partial^2 u_3}{\partial x_1 \partial x_3}\right) + c_3^2\left(\frac{\partial^2 u_1}{\partial^2 x_2^2} + \frac{\partial^2 u_2}{\partial x_1 \partial x_2} + \frac{\partial^2 u_1}{\partial x_3^2} + \frac{\partial^2 u_3}{\partial x_1 \partial x_3}\right) = \frac{\partial^2 u_1}{\partial t^2}, \tag{2.9}$$

$$(c_3^2 + c_4^2)\frac{\partial^2 u_1}{\partial x_1 \partial x_2} + c_3^2 \frac{\partial^2 u_2}{\partial x_1^2} + c_1^2 \frac{\partial^2 u_2}{\partial x_2^2} + c_2^2 \frac{\partial^2 u_2}{\partial x_3^2} + (c_1^2 - c_2^2)\frac{\partial^2 u_3}{\partial x_2 \partial x_3} = \frac{\partial^2 u_2}{\partial t^2}, \tag{2.10}$$

$$c_3^2\left(\frac{\partial^2 u_1}{\partial x_3 \partial x_1} + \frac{\partial^2 u_3}{\partial x_1^2}\right) + c_2^2\left(\frac{\partial^2 u_2}{\partial x_2 \partial x_3} + \frac{\partial^2 u_3}{\partial x_2^2}\right) + c_4^2 \frac{\partial^2 u_1}{\partial x_1 \partial x_3} + (c_1^2 - 2c_2^2)\frac{\partial^2 u_2}{\partial x_2 \partial x_3}$$

$$+ c_1^2 \frac{\partial^2 u_3}{\partial x_2^2} = \frac{\partial u_3}{\partial t^2}, \tag{2.11}$$

within which c_1^2, c_2^2, c_3^2, c_4^2 and c_5^2 are defined by

$$\rho c_1^2 = \lambda + 2\mu_T, \qquad \rho c_2^2 = \mu_T, \rho c_3^2 = \mu_L,$$

$$\rho c_4^2 = \lambda + \alpha, \qquad \rho c_5^2 = \lambda + 4\mu_L - 2\mu_T + 2\alpha + \beta. \tag{2.12}$$

The traction-free boundary conditions (2.2) are now expressible in the form

$$\frac{\partial u_1}{\partial x_3}+\frac{\partial u_3}{\partial x_1}=0, \qquad \frac{\partial u_2}{\partial x_3}+\frac{\partial u_3}{\partial x_2}=0, \qquad c_4^2\frac{\partial u_1}{\partial x_1}+(c_1^2-2c_2^2)\frac{\partial u_2}{\partial x_2}+c_1^2\frac{\partial u_3}{\partial x_3}$$

$$\text{at } x_3=\pm h. \tag{2.13}$$

Solutions of the equations of motion are now sought in the form of the travelling waves

$$\mathbf{u}=(U, V, W)\mathrm{e}^{kqx_3}\mathrm{e}^{\mathrm{i}k(x_1-vt)}. \tag{2.14}$$

Utilizing equation (2.14) in equations (2.9)–(2.11) the three components of the equations of motion are expressible in the form

$$(v^2-c_5^2+q^2c_3^2)U+\mathrm{i}q(c_3^2+c_4^2)W=0, \tag{2.15}$$

$$(v^2-c_3^2+c_2^2q^2)V=0, \tag{2.16}$$

$$\mathrm{i}q(c_3^2+c_4^2)U+(v^2-c_3^2+q^2c_1^2)W=0. \tag{2.17}$$

The correspondidng traction-free boundary conditions, to be satisfied at the upper and lower surfaces of the plate, are similarly obtainable and take the form

$$qU+\mathrm{i}W=0, \qquad qV=0, \qquad \mathrm{i}(\lambda+\alpha)U+q(\lambda+2\mu_T)W=0$$

$$\text{at } x_3=\pm h. \tag{2.18}$$

It is observed from the equations of motion that the equation for V uncouples from those involving U and W. Moreover, the boundary condition $(2.13)_2$ is satisfied provided

$$\rho v^2=c_3^2+\frac{(2n+1)^2\pi^2}{4(kh)^2} \text{ or } \rho v^2=c_3^2+\frac{n^2\pi^2}{(kh)^2}, \tag{2.19}$$

corresponding to anti-symmetric and symmetric modes respectively. The dispersion relations (2.19) are those associated with horizontally polarized shear waves, usually referred to as *SH* waves. It is also noted that $(2.13)_2$ is also satisfied when $q=0$. This represents a non-dispersive shear wave travelling with a constant speed $v=c_3$ which will leave any plane $x_3=$ *constant* traction free. Such waves are usually termed exceptional and are important in the theory of surface waves and body wave reflections at boundaries [14].

The two other equations of motion (2.9) and (2.11) will have a non-trivial solution provided

$$c_1^2c_3^2q^4+\{c_1^2(v^2-c_5^2)+c_3^2(v^2-c_3^2)+(c_3^2+c_4^2)^2\}q^2+(v^2-c_5^2)(v^2-c_3^2)=0. \tag{2.20}$$

If the two solutions of equation (2.20) are denoted by q_1^2 and q_2^2 it is readily deduced for future reference that

$$q_1^2 + q_2^2 = \frac{c_1^2(c_5^2 - v^2) + c_3^2(c_3^2 - v^2) - (c_3^2 + c_4^2)^2}{c_1^2 c_3^2}, \tag{2.21}$$

$$q_1^2 q_2^2 = \frac{(v^2 - c_5^2)(v^2 - c_3^2)}{c_1^2 c_3^2} \tag{2.22}$$

and solutions for U and W are obtainable as linear combinations of the four solutions of equation (2.20) in the form

$$U = \left(\sum_{m=1}^{4} \frac{-\mathrm{i}F(q_m)}{q_m} W^{(m)} \mathrm{e}^{kq_m x_3} \right) \mathrm{e}^{\mathrm{i}k(x_1 - vt)}, \tag{2.23}$$

$$W = \left(\sum_{m=1}^{4} W^{(m)} \mathrm{e}^{kq_m x_3} \right) \mathrm{e}^{\mathrm{i}k(x_1 - vt)} \tag{2.24}$$

in which

$$F(q) = \frac{c_3^2 - v^2 - c_1^2 q^2}{c_3^2 + c_4^2}. \tag{2.25}$$

The dispersion relation is derived by assuming that the plate is traction free at the two surfaces $x_3 = \pm h$. Accordingly, equations (2.15) and (2.17) may be used in conjunction with $(2.18)_{1,3}$ to obtain the following system of homogeneous equations:

$$G(q_1)W^{(1)}E_1^+ + G(q_1)W^{(2)}E_1^- + G(q_2)W^{(3)}E_2^+ + G(q_2)W^{(4)}E_2^- = 0, \tag{2.26}$$

$$G(q_1)W^{(1)}E_1^- + G(q_1)W^{(2)}E_1^+ + G(q_2)W^{(3)}E_2^- + G(q_2)W^{(4)}E_2^+ = 0, \tag{2.27}$$

$$\frac{H(q_1)}{q_1} W^{(1)}E_1^+ - \frac{H(q_1)}{q_1} W^{(2)}E_1^- + \frac{H(q_2)}{q_2} W^{(3)}E_2^+ - \frac{H(q_2)}{q_2} W^{(2)}E_2^- = 0, \tag{2.28}$$

$$\frac{H(q_1)}{q_1} W^{(1)}E_1^- - \frac{H(q_1)}{q_1} W^{(2)}E_1^+ + \frac{H(q_2)}{q_2} W^{(3)}E_2^- - \frac{H(q_2)}{q_2} W^{(2)}E_2^+ = 0, \tag{2.29}$$

in which

$$G(q) = 1 - F(q), \quad H(q) = c_4^2 F(q) + c_1^2 q^2, \quad E_i^+ = \mathrm{e}^{kq_i h}, \quad E_i^- = \mathrm{e}^{-kq_i h}. \tag{2.30}$$

If equations (2.26) and (2.27) are added and equations (2.28) and (2.29) subtracted we obtain a system of two equations in $(W^{(1)} + W^{(2)})$, whilst if equations (2.26) and (2.27) are subtracted and equations (2.28) and (2.29) added a system of two equations in $(W^{(1)} - W^{(2)})$ is obtained. System (2.26)–(2.29) may then be decomposed into the two systems

$$G(q_1)(W^{(1)} + W^{(2)})\mathrm{Cosh}(kq_1 h) + G(q_2)(W^{(3)} + W^{(4)})\mathrm{Cosh}(kq_2 h) = 0, \tag{2.31}$$

$$\frac{H(q_1)}{q_1}(W^{(1)} + W^{(2)})\mathrm{Sinh}(kq_1 h) + \frac{H(q_2)}{q_2}(W^{(3)} + W^{(4)})\mathrm{Sinh}(kq_2 h) = 0, \tag{2.32}$$

or

$$G(q_1)(W^{(1)} - W^{(2)})\,\mathrm{Sinh}(kq_1h) + G(q_2)(W^{(3)} - W^{(4)})\mathrm{Sinh}(kq_2h) = 0, \quad (2.33)$$

$$\frac{H(q_1)}{q_1}(W^{(1)} - W^{(2)})\,\mathrm{Cosh}(kq_1h) + \frac{H(q_2)}{q_2}(W^{(3)} - W^{(4)})\mathrm{Cosh}(kq_2h) = 0. \quad (2.34)$$

It is readily deduced from equations (2.31) and (2.32) that a non-trivial solution will exist provided

$$(c_1^2q_1^2 + v^2 + c_4^2)(c_1^2c_3^2q_2^2 - c_4^2(v^2 - c_3^2))\frac{\mathrm{Tanh}(kq_2h)}{q_2}$$

$$= (c_1^2q_2^2 + v^2 + c_4^2)(c_1^2c_3^2q_1^2 - c_4^2(v^2 - c_3^2))\frac{\mathrm{Tanh}(kq_1h)}{q_1} \quad (2.35)$$

with a similar non-trivial solution of equations (2.33) and (2.34) existing provided

$$(c_1^2q_1^2 + v^2 + c_4^2)(c_1^2c_3^2q_2^2 - c_4^2(v^2 - c_3^2))\frac{\mathrm{Tanh}(kq_1h)}{q_2}$$

$$= (c_1^2q_2^2 + v^2 + c_4^2)(c_1^2c_3^2q_1^2 - c_4^2(v^2 - c_3^2))\frac{\mathrm{Tanh}(kq_2h)}{q_1} \quad (2.36)$$

It is noted that the u_3 associated with equations (2.35) and (2.36) are odd and even about the mid-plane, respectively. It follows that (2.35) is the dispersion relation associated with extensional waves, whilst equation (2.36) is concerned with flexural (or bending) waves. The dispersion relation (2.35) was seemingly first derived in reference [1], which contains a detailed analysis of the inextensible limit but numerical results in respect of only the first few harmonics and little asymptotic analysis.

3. HIGH WAVE NUMBER ASYMPTOTIC INVESTIGATION

3.1. THE HARMONICS

Numerical results indicate that for high wave number and strong anisotropy all harmonics of equations (2.35) and (2.36) have one of q_1, q_2 purely imaginary with a modulus which tends to zero as $kh \to \infty$, the other remaining real and finite. Accordingly as $kh \to \infty$

$$q_1 = \mathrm{i}\hat{q}_1, \qquad \hat{q}_1 \sim 0, \qquad q_2^2 \approx \frac{c_1^2(c_5^2 - c_3^2) - (c_3^2 + c_4^2)^2}{c_3^2c_2^2} \quad (3.1)$$

from which we are able to deduce that q_2 is real provided

$$c_5^2 > \frac{(c_3^2 + c_4^2)^2 + c_1^2c_3^2}{c_1^2}, \quad (3.2)$$

a requirement certainly met for highly anisotropic material, for which we recall that $c_5 \gg \max(c_1, c_2, c_3, c_4)$.

It is of interest to briefly digress and discuss the case in which the material is not strongly anisotropic and (3.2) is violated, c_5 then being the same order of magnitude as all other material parameters. At first sight it may appear from equation (2.20) that the requirement $\hat{q} \sim 0$ as $kh \to \infty$ implies that it is possible that $v = c_5$ is a possible high wave number limiting wave speed of the harmonics. It can easily be shown however that this is not a possible limit as q_2 cannot have a real limiting value. The asymptotic behaviour in such cases is more complicated and will be explicated elsewhere.

The high wave number representation of the dispersion relation (2.35) is therefore given by

$$\begin{aligned}&(-c_1^2\hat{q}_1^2 + v^2 + c_4^2)(c_1^2c_3^2q_2^2 - c_4^2(v^2 - c_3^2))\frac{1}{q_2}\\ &= (c_1^2q_2^2 + v^2 + c_4^2)(-c_1^2c_3^2\hat{q}_1^2 - c_4^2(v^2 - c_3^2))\frac{\tan(k\hat{q}_1h)}{\hat{q}_1}.\end{aligned} \tag{3.3}$$

From equation (3.3) it is deduced that as $kh \to \infty$ and $\hat{q}_1 \to 0$, $\tan(k\hat{q}_1h) \sim \hat{q}_1^{-1}$, and therefore

$$\tan(k\hat{q}_1h) \gg 1 \Rightarrow k\hat{q}_1h \approx \frac{(2n+1)\pi}{2}. \tag{3.4}$$

Utilizing equation (2.20) and assuming that $\hat{q}_1$ is small yields

$$v^2 = c_3^2 + \left(\frac{c_1^2(c_5^2 - c_3^2) - (c_3^2 + c_4^2)^2}{c_5^2 - c_3^2}\right)\hat{q}_1^2 + \mathrm{O}(\hat{q}_1^4). \tag{3.5}$$

Motivated by the form of $\hat{q}_1$ shown in equation (3.4) we seek to improve the approximation obtainable for the phase speed associated with each harmonic in the high wave number regime by setting

$$k\hat{q}_1h = \left(n + \frac{1}{2}\right)\pi + \frac{\phi}{kh} + \mathrm{O}(kh)^2 \Rightarrow \tan(k\hat{q}_1h) = -\frac{kh}{\phi} + \mathrm{O}(1) \tag{3.6}$$

in which ϕ is an O(1) quantity to be determined. It is possible to obtain an expression for ϕ by inserting equation (3.6) into equation (3.3) and then equating leading order terms, to yield

$$\phi = \left(\frac{\hat{q}_2(c_1^2\hat{q}_2^2 + c_3^2 + c_4^2)(c_3^2c_2^2(c_3^2 - c_5^2) + c_4^2(c_1^2(c_3^2 - c_5^2) + (c_3^2 + c_4^2)^2}{c_1^2c_3^2(c_4^2 + c_3^2)(c_3^2 - c_5^2)\hat{q}_2^2}\right)\left(n + \frac{1}{2}\right)\pi \tag{3.7}$$

in which $\hat{q}_2$ is the appropriate leading order approximation for q_2, given by

$$\hat{q}_2 = \sqrt{\frac{c_1^2(c_3^2 - c_5^2) - (c_3^2 + c_4^2)^2}{c_1^2c_3^2}}. \tag{3.8}$$

It is now possible to establish that

$$v^2 = c_3^2 + \left(\frac{c_1^2(c_3^2 - c_5^2) + (c_3^2 + c_4^2)^2}{c_3^2 - c_5^2}\right)\left(\frac{(2n+1)\pi}{2kh}\right)^2\left(1 + \frac{2\hat{\phi}}{kh}\right) + \mathrm{O}(kh)^4 \quad (3.9)$$

in which

$$\hat{\phi} = \frac{2\phi}{(2n+1)\pi}.$$

We now turn our attention to the flexural wave dispersion relation (2.36) which may be recast in the appropriate high wave number representation

$$(-c_1^2\hat{q}_1^2 + v^2 + c_4^2)(c_1^2c_3^2q_2^2 - c_4^2(v^2 - c_3^2))\frac{\tan(k\hat{q}_1h)}{q_2}$$

$$= \frac{(c_1^2q_2^2 + v^2 + c_4^2)}{\hat{q}_1}(-c_1^2c_3^2\hat{q}_1^2 - c_4^2(v^2 - c_3^2)). \quad (3.10)$$

from which it is deduced that as $kh \to \infty$, $\tan(k\hat{q}_1) \ll 1$, and accordingly we assume that

$$k\hat{q}_1h = n\pi + \frac{\eta}{kh} + \mathrm{O}(kh)^{-2} \Rightarrow \tan(k\hat{q}_1h) = \frac{\eta}{kh} + \mathrm{O}(kh)^{-2}. \quad (3.11)$$

If equation (3.11) is now inserted into equation (3.10) and leading order terms in kh equated we obtain

$$\eta = \left(\frac{\hat{q}_2(c_1^2\hat{q}_2^2 + c_3^2 + c_4^2)(c_3^2c_2^2(c_3^2 - c_5^2) + c_4^2(c_1^2(c_3^2 - c_5^2) + (c_3^2 + c_4^2)^2}{c_1^2c_3^2(c_4^2 + c_3^2)(c_3^2 - c_5^2)\hat{q}_2^2}\right)n\pi. \quad (3.12)$$

Utilization of equations (3.11) and (3.12) with equation (2.20) reveals that the high wave number representation of the phase speed of all harmonics associated with flexural motion is given by

$$v^2 = c_3^2 + \left(\frac{c_1^2(c_3^2 - c_5^2) + (c_3^2 + c_4^2)^2}{c_3^2 - c_5^2}\right)\left(\frac{n\pi}{kh}\right)^2\left(1 + \frac{2\hat{\eta}}{2kh}\right) + \mathrm{O}(kh)^4 \quad (3.13)$$

in which

$$\hat{\eta} = \frac{\eta}{n\pi}.$$

3.2. THE FUNDAMENTAL MODE

For the fundamental mode of either equation (2.35) or equation (2.36) both q_1 and q_2 are real or form a complex conjugate pair. The high wave number limit of either of these two dispersion relations is therefore obtainable by replacing the

hyperbolic tangents by unity, to yield in either case

$$c_1^4 c_3^2 (v^2 - c_5^2)(v^2 - c_3^2) - c_1^2 (v^2 c_3^2) c_4^2 (c_1^2 (c_5^2 - v^2) + c_3^2 (c_3^2 - v^2) - (c_3^2 + c_4^2)^2)$$
$$+ c_1 c_3 ((v^2 + c_4^2) c_1^2 c_3^2 - c_1^2 (v^2 - c_3^2) c_4^2) \sqrt{(v^2 - c_5^2)(v^2 - c_3^2)}$$
$$- c_4^2 (v^2 - c_3^2)(v^2 - c_4^2) c_3^2 c_1^2 = 0. \tag{3.14}$$

Equation (3.14) is the Rayleigh surface wave speed equation. From this equation the speed of propagation of the surface wave propagating in a half-space composed to transversely isotropic elastic material may be obtained. This equation has previously been obtained and the existence of such waves discussed in detail [2].

4. LOW WAVE NUMBER ASYMPTOTIC INVESTIGATION

4.1. THE HARMONICS

Numerical investigation reveals that in the low wave number limit $\rho v^2 \to \infty$ as $kh \to 0$ for all harmonics. Accordingly, equation (2.20) may be used to establish that in the low wave number (long wave) region

$$q_1^2 = -\frac{v^2}{c_1^2} + \bar{q}_1^2 + \mathrm{O}(v^{-2}), \qquad q_2^2 = -\frac{v^2}{c_3^2} + \bar{q}_2^2 + \mathrm{O}(v^{-2}), \tag{4.1}$$

within which

$$\bar{q}_1^2 = \frac{(c_3^2 + c_4^2)^2 + c_3^2 (c_1^2 - c_3^2)}{c_1^2 (c_1^2 - c_3^2)}, \qquad \bar{q}_2^2 = -\frac{(c_3^2 + c_4^2)^2 + c_5^2 (c_1^2 - c_3^2)}{c_3^2 (c_1^2 - c_3^2)}. \tag{4.2}$$

For future use it is noted that q_1 and q_2 may be expressed in the form $q_1 = \mathrm{i}\hat{q}_1$ and $q_2 = \mathrm{i}\hat{q}_2$, where

$$\hat{q}_1 = \frac{v}{c_1}\left(1 - \frac{\bar{q}_1^2 c_1^2}{2v^2}\right) + \mathrm{O}(v^{-2}), \quad \hat{q}_2 = \frac{v}{c_3}\left(1 - \frac{\bar{q}_2^2 c_3^2}{2v^2}\right) + \mathrm{O}(v^{-2}). \tag{4.3}$$

Utilizing equations (4.1) in equation (2.35) it is readily established that for extensional harmonics in the long wave regime

$$\mathscr{A}_1 \tan(k\hat{q}_1 h) \sim \mathscr{A}_2 \tan(k\hat{q}_2 h) v^2, \tag{4.4}$$

$$\mathscr{A}_1 = c_3 (c_4^2 + c_1^2 \bar{q}_1^2)(c_1^2 + c_4^2), \qquad \mathscr{A}_2 = c_1 (c_3^2 + c_4^2)\left(1 - \frac{c_1^2}{c_3^2}\right),$$

implying that

$$\tan(k\hat{q}_1 h) \sim \mathrm{O}(v^2) \text{ or } \tan(k\hat{q}_2 h) \sim \mathrm{O}(v^{-2}). \tag{4.5}$$

The first case, equation $(4.5)_1$ implies that $\tan(k\hat{q}_1 h) \gg 1$ and therefore we assume that

$$k\hat{q}_1 h = (n + \tfrac{1}{2})\pi + \gamma_1 (kh)^2 + \mathrm{O}(kh)^3 \Rightarrow \tan(k\hat{q}_1 h) = -\frac{1}{\gamma_1 (kh)^2} + \mathrm{O}(1), \tag{4.6}$$

in which γ_1 is an O(1) quantity to be determined. Equation (4.6) may now be inserted into equation (4.4) to establish that

$$k\hat{q}_2 h = (n + \tfrac{1}{2})\pi c_1 c_3^{-1} + \mathrm{O}(kh)^2,$$

thus enabling γ_1 to be found by equating leading order terms in equation (4.4), yielding

$$\gamma_1 = -\frac{\mathscr{A}_1}{\mathscr{A}_2 \Lambda_1^2 \tan(\Lambda_1 c_3^{-1})}, \qquad \Lambda_1 = (n + \tfrac{1}{2})\pi c_1. \tag{4.7}$$

This expression for γ_1 may now be first inserted into equation (4.6) and then into equation $(4.3)_1$ to obtain the appropriate phase-speed expansion

$$v^2 = \frac{\Lambda_1^2}{(kh)^2} + \bar{q}_1^2 c_1^2 + \frac{2\mathscr{A}_1 c_3}{\mathscr{A}_2 \Lambda_1 \tan(\Lambda_1 c_3^{-1})} + \mathrm{O}(kh)^2. \tag{4.8}$$

The second possible case indicated in equation (4.5) may be used to infer that

$$\hat{q}_2 = \frac{n\pi}{kh} + \gamma_2(kh) + \mathrm{O}(kh)^2 \Rightarrow \tan(k\hat{q}_2 h) = \gamma_2(kh)^2 \mathrm{O}(kh)^4, \qquad \hat{q}_1 = \frac{c_3 n\pi}{khc_1} + \mathrm{O}(kh). \tag{4.9}$$

Equation (4.9) may now be used in conjunction with equation (4.4) to establish that

$$\gamma_2 = \frac{\mathscr{A}_1 \tan(\Lambda_2 c_1^{-1})}{\mathscr{A}_2 \Lambda_2^2}, \qquad \Lambda_2 = n\pi c_3 \tag{4.10}$$

which may be used with equation $(4.3)_2$ to obtain the phase-speed expansion

$$v^2 = c_3^2 \left(\frac{\Lambda_2}{kh}\right)^2 + c_3^2 \bar{q}_2^2 + \left(\frac{2\mathscr{A}_1 c_3 \tan(\Lambda_2 c_1^{-1})}{\mathscr{A}_2 \Lambda_2}\right) + \mathrm{O}(kh)^2. \tag{4.11}$$

In the case of flexural waves the analogous form of equation (4.5) is

$$\mathscr{A}_1 \tan(k\hat{q}_2 h) \sim \mathscr{A}_2 \tan(k\hat{q}_1 h) v^2 \tag{4.12}$$

implying that

$$\tan(k\hat{q}_2 k) \sim \mathrm{O}(v^2) \text{ or } \tan(k\hat{q}_1 k) \sim \mathrm{O}(v^{-2}). \tag{4.13}$$

Equation $(4.13)_1$ is now employed to establish that

$$k\hat{q}_2 h = (n + \tfrac{1}{2})\pi + \gamma_3(kh)^2 + \mathrm{O}(kh)^3 \Rightarrow \tan(k\hat{q}_2 \mathrm{h}) = -\frac{1}{\gamma_3(kh)^2} + \mathrm{O}(1) \tag{4.14}$$

and

$$k\hat{q}_1 h = (n + \tfrac{1}{2})\frac{\pi c_3}{c_1} + \mathrm{O}(kh)^2 \Rightarrow \tan(k\hat{q}_1 h) = \tan\left((n + \tfrac{1}{2})\frac{\pi c_3}{c_1}\right) + \mathrm{O}(kh)^2. \tag{4.15}$$

Equations (4.14) and (4.15) may now be inserted into (4.12), and leading orders of kh equated, to obtain

$$\gamma_3 = -\frac{\mathscr{A}_1}{\mathscr{A}_2 \tan(\Lambda_3 c_1^{-1})\Lambda_3^2}, \quad \Lambda_3 = (n + \tfrac{1}{2})\pi c_3. \tag{4.16}$$

This expression for γ_3 may now be used in equations $(4.14)_1$ and $(4.3)_2$ to obtain the low wave number expansion

$$v^2 = \frac{\Lambda_3^2}{(kh)^2} + \bar{q}_2^2 c_3^2 - \frac{2\mathscr{A}_1 c_3}{\mathscr{A}_2 \tan(\Lambda_3 c_1^{-1})\Lambda_3} + \mathrm{O}(kh)^2. \tag{4.17}$$

We now consider the second case, equation $(4.13)_2$, for which

$$k\hat{q}_1 h = n\pi + \gamma_4 (kh)^2 + \mathrm{O}(kh)^3 \Rightarrow \tan(k\hat{q}_1 h) = \gamma_4 (kh)^2 + \mathrm{O}(kh)^4 \tag{4.18}$$

and

$$k\hat{q}_2 h = \frac{n\pi c_1}{c_3} + O(kh)^2 \Rightarrow \tan(k\hat{q}_2 h) = \tan\left(\frac{n\pi c_1}{c_3}\right) + \mathrm{O}(kh)^2. \tag{4.19}$$

Equations (4.18) and (4.19) may now be inserted into equation (4.12) and like powers of kh equated to show that

$$\gamma_4 = \frac{\mathscr{A}_1 \tan(\Lambda_4 c_3^{-1})}{\mathscr{A}_2 \Lambda_4^2}, \qquad \Lambda_4 = n\pi c_1, \tag{4.20}$$

which by using equation $(4.3)_1$ enables us to obtain

$$v^2 = \left(\frac{\Lambda_4}{kh}\right)^2 + c_1^2 \bar{q}_1^2 + \frac{2c_1 \mathscr{A}_1 \tan(\Lambda_4 c_3^{-1})}{\mathscr{A}_2 \Lambda_4} + \mathrm{O}(kh)^2. \tag{4.21}$$

The expansions just derived are the so-called long-wave high-frequency approximations. Moreover, $\Lambda_1, \Lambda_2, \Lambda_3$ and Λ_4 are the appropriate cut-off frequencies associated with symmetric and anti-symmetric stretch and shear resonance. These long wave high-frequency approximations have direct relevance to acoustic scattering and radiation [15].

4.2. THE FUNDAMENTAL MODE

Finally, in this section we consider the long-wave ($kh \to 0$) limiting phase speed of the fundamental mode which may be obtained from equations (2.35) and (2.36) by replacing the hyperbolic tangents by their arguments. The limiting speeds of extensional and flexural fundamental modes, denoted by $v^f(0)$ and $v^e(0)$, respectively, are then found to be given by

$$v^f(0) = 0, \qquad v^e(0) = \sqrt{\frac{c_1^2 c_5^2 - c_4^4}{c_1^2}}. \tag{4.22}$$

5. NUMERICAL RESULTS

In this section some numerical results are presented and discussed. In all the figures presented in this section data is employed which has been measured for a carbon fibre-epoxy resin composite, see reference [16]. The values of c_1, c_2, c_3, c_4 and c_5 are thus given by

$$\rho c_1^2 = 10{\cdot}57 \times 10^9 \text{ Nm}^{-2}, \qquad \rho c_2^2 = 2{\cdot}46 \times 10^9 \text{ Nm}^{-2}, \qquad \rho c_3^2 = 5{\cdot}66 \times 10^9 \text{ Nm}^{-2},$$
$$\rho c_4^2 = 4{\cdot}37 \times 10^9 \text{ Nm}^{-2}, \qquad \rho c_5^2 = 241{\cdot}71 \times 10^9 \text{ Nm}^{-2}. \tag{5.1}$$

In Figures 1 and 2 numerical solutions of the dispersion relation (2.35), fundamental mode and first 50 harmonics for extensional waves are presented. Specifically, Figure 1 shows scaled phase speed against scaled wave number, with Figure 2 showing the corresponding plot of frequency against kh. A significant feature observed in Figure 1 is the distinct flattening of the harmonics around the value $v = c_5 \approx 15{\cdot}55$. A corresponding striking feature of Figure 2 in the ghost line brought about by the oscillation of the harmonic branches. This ghost line has a gradient $\omega/kh = c_5$. As the dispersion curves approach the ghost line from the left they exhibit the well-known *plateau* and *step* phenomenon. Along the plateau the curves are almost parallel to the ghost line with phase speed almost constant. After crossing the ghost line all branches are virtually parallel, with gradient $\omega/kh = c_3$, the high wave number limit of all harmonics. This flattering of the harmonics in Figure 1, or ghost line associated with Figure 2, will give rise to a longitudinal wave front travelling with a speed of $v = c_5$, made up of the cumulative effect of all the harmonics and the contribution from each harmonic occurrs in adjacent wave number regimes. It is then expected that there are two body wave fronts. The first associated with the high wave number limit of all harmonics, termed the first wave

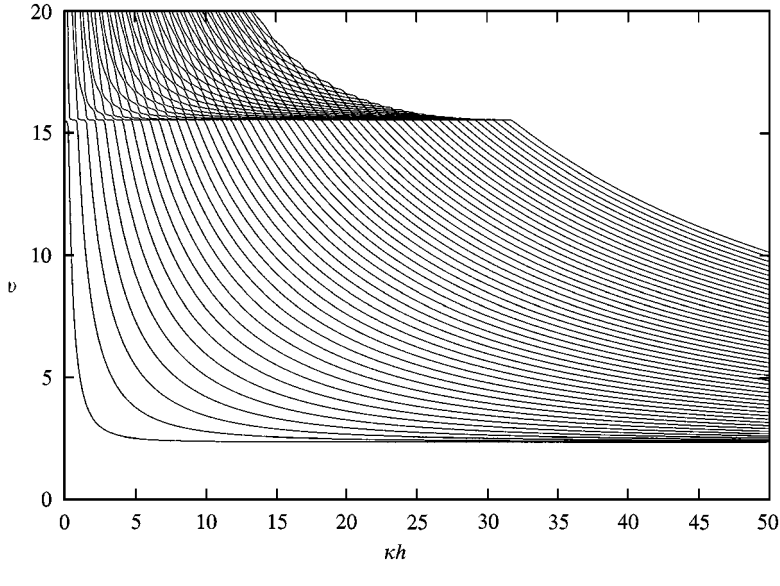

Figure 1. Numerical solutions of the dispersion relation showing v against kh, extensional waves.

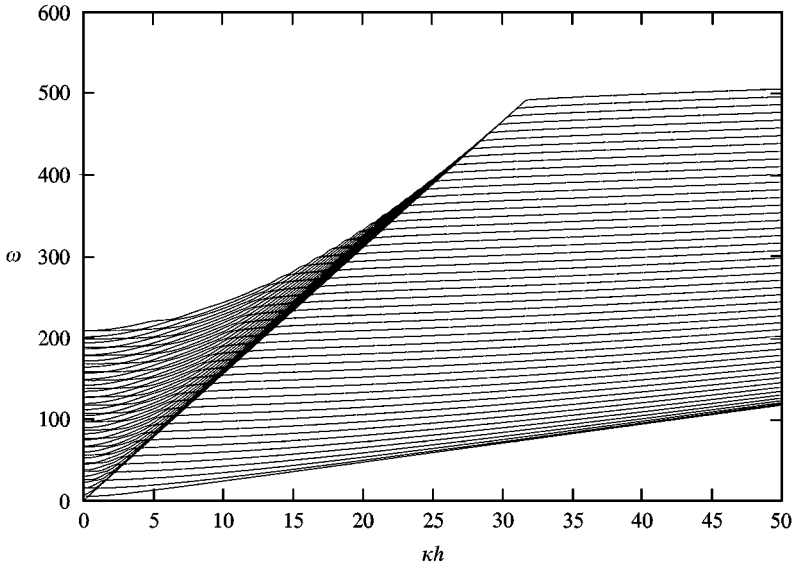

Figure 2. Numerical solutions of the dispersion relation showing ω against kh, extensional waves.

front and travelling with a speed given by $\rho v^2 = c_3$ and this second wave front with a speed of $\rho v^2 = c_5$.

The high wave number phase speed limit of the harmonics is only really evident for the first few harmonics. Notwithstanding this it has been verified numerically that for all the harmonics in Figure 1 $v \to c_3$ from above as $kh \to \infty$. Other features which are consistent with earlier observations are (i) the wave speed associated with the fundamental mode tends to a non-zero limit, see equation $(4.22)_2$, (ii) for all harmonics $v \to \infty$ as $kh \to 0$ and (iii) the high wave number limit of fundamental mode is the associated Rayliegh surface wave speed. It is also noted that as $kh \to 0$ all branches of the frequency–wave number curves shown in Figure 2 exhibit non-zero cut-off frequencies, with the exception of the fundamental mode.

Although the nature of a pulse is determined by the phase velocity, it is well known that for dispersive waves the parameter which governs the motion of a pulse is the group velocity v_g. This is defined as the gradient of the frequency curves, thus $v_g = \partial\omega/\partial k$. In Figure 3 a plot of the scaled group velocity v_g against kh is presented, showing the fundamental mode and first nine harmonics. Some of the most notable features of this graph are the local maxima associated with each harmonic at $v_g = c_5$. It is well-known that long time transient response usually decays like $t^{-1/2}$; however, at local turning points of the group velocity curves the decay is more slowly, like $t^{-1/3}$. Such maxima may then yield a significant contribution to transient response.

In Figures 4–6 the corresponding curves for flexural waves are presented. The observations and conclusions from these graphs are similar to those already discussed in the context of extensional waves. However, slight qualitative differences do occur and it is first noted that the low wave number phase speed limit

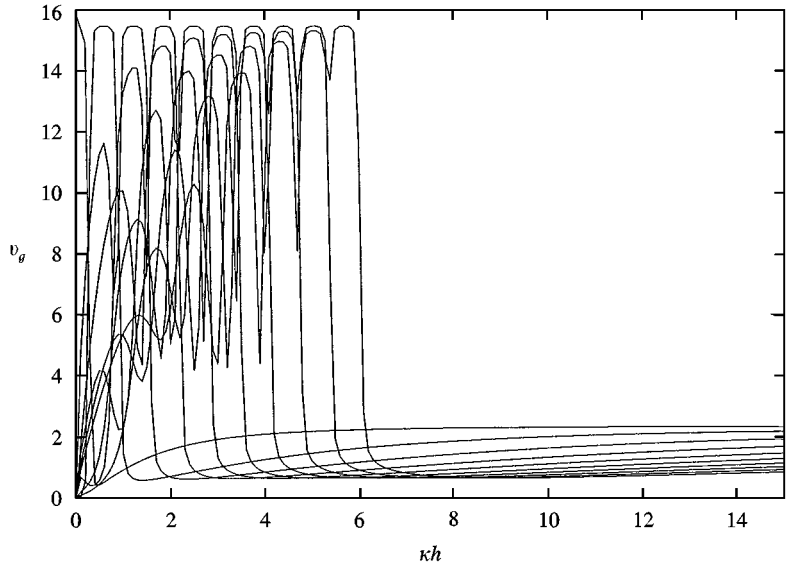

Figure 3. Group velocity curves showing v_g against kh, extensional waves.

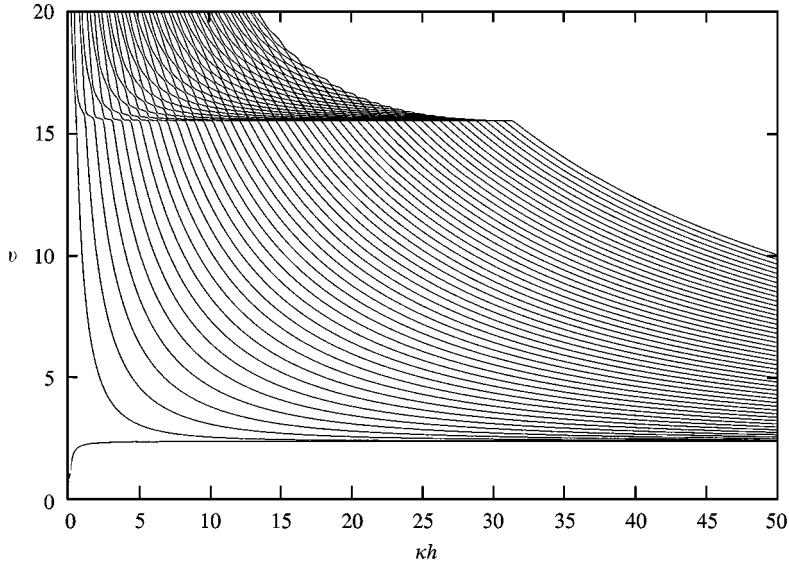

Figure 4. Numerical solutions of the dispersion relation showing v against kh, flexural waves.

of the fundamental mode is zero. A further point of interest is that the flattening of the harmonics around $v = c_5$ is not as sharp for the first few harmonics as it is in the case of extensional waves. The implication is that the first few maxima of the associated group velocity curves shown in Figure 6 are slightly below $v_g = c_5$. Finally, in this section, in Figures 7 and 8 comparison of numerical solution with the asymptotic high wave number approximations (3.9) and (3.13) is made.

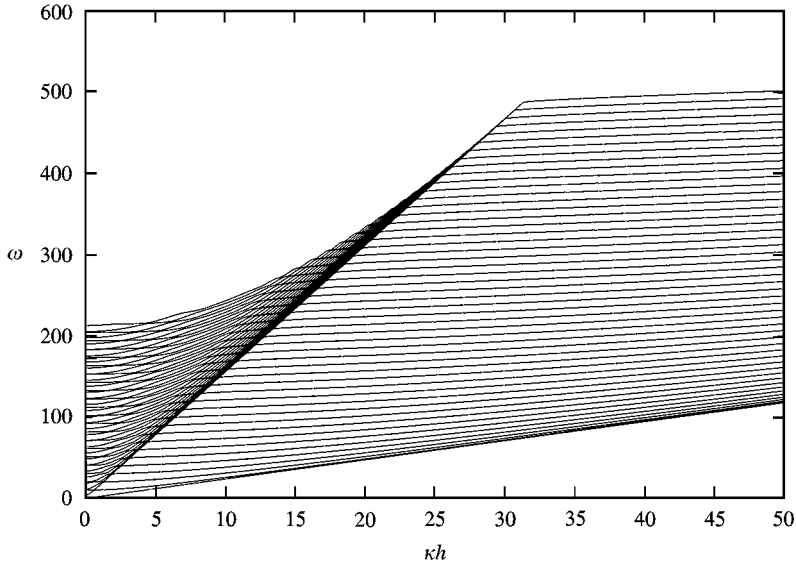

Figure 5. Numerical solutions of the dispersion relation showing ω against kh, flexural waves.

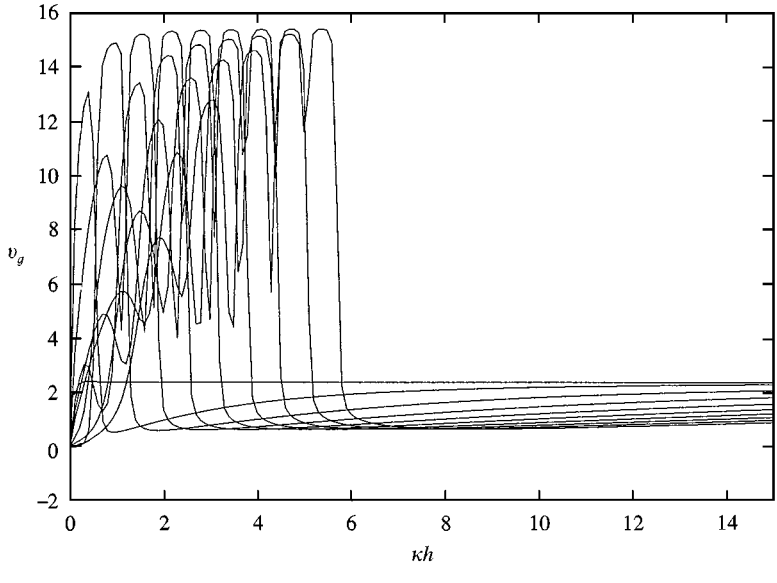

Figure 6. Group velocity curves showing v_g against kh, flexural waves.

These two graphs show quite remarkable agreement between the asymptotic and numerical solutions.

6. SOME COMMENTS ABOUT THE SECOND (LONGITUDINAL) WAVE FRONT

It has already been observed in the previous section that a wave front is formed from the cumulative effect of the harmonics and travels with a speed $v = c_5$.

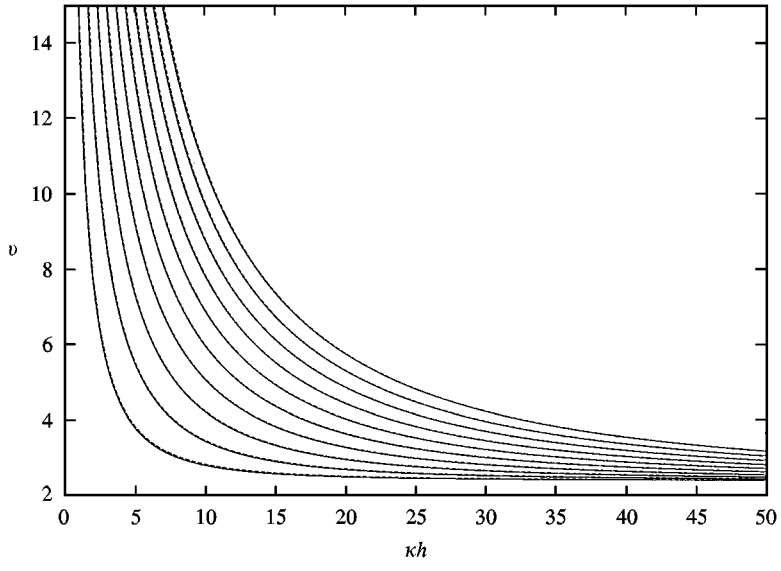

Figure 7. Comparison of numerical solutions with asymptotic expansions, showing phase speed against kh for extensional waves. Numerical solutions —; Asymptotic expansions - - - .

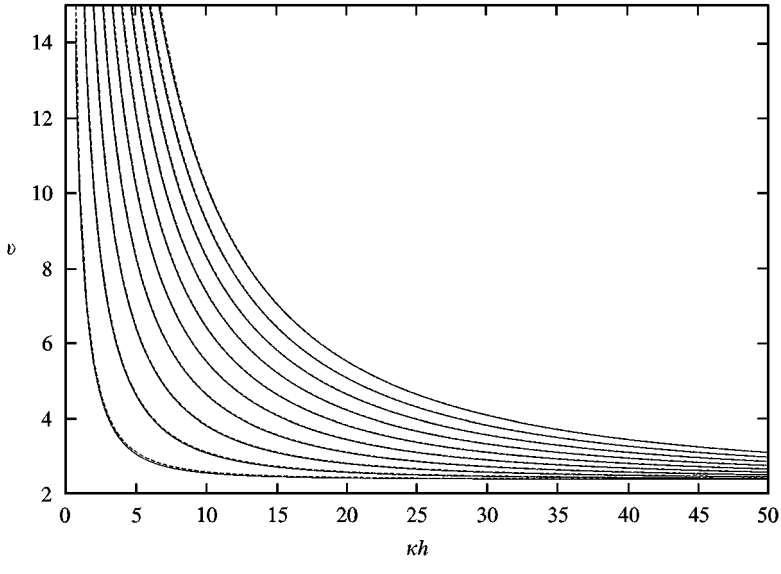

Figure 8. Comparison of numerical solutions with asymptotic expansions, showing phase speed against kh for flexural waves. Numerical solutions —; Asymptotic expansions - - - .

Moreover, this speed is the same order as the Young's modulus and as the inextensible limit in the fibre direction is reached the speed of the associated wave will tend to infinity. To elucidate this wave in the case of large Young's modulus the dispersion relation for flexural waves is plotted in Figure 9 for the case $c_5^2 = 5000{\cdot}0$. In this Figure a wave front is clearly evident at $v \approx 71{\cdot}0$. The nature of the wave

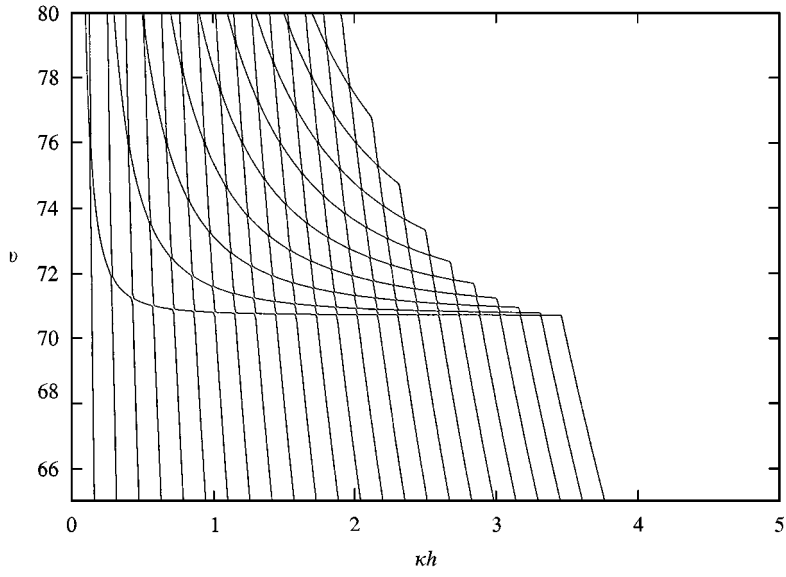

Figure 9. Numerical solutions of the dispersion relation showing v against kh, extensional waves, when $c_5^2 = 5000{\cdot}0$.

motion associated with this wave is interesting. It has already been remarked that the associated wave speed will tend to infinity as the material approaches the inextensible limit. This is essentially an indication of increasing material rigidity. Moreover, it has been shown for a simple boundary value problem that such a wave will, in the inextensible limit, have infinite speed, zero amplitude and infinite wavelength [17].

In Figure 10 a plot of the group velocity associated with the dispersion curves in Figure 9 is presented. In this plot distinct maxima are shown and at first glance the plots look very similar to those previously discussed in respect of Figures 3 and 6. A significant difference however is the wave number scale. In this case the scale is small and it is conjectured that the first few harmonics, which are dominant in determining transient response, have maximums over too small wave number to make a significant contribution to any wave front. It is therefore conjectured that the amplitude of the wave front travelling with speed $v_2 = c_5$ will decrease as the material becomes inextensible in the fibre direction. Numerical calculation are currently being carried out to substantiate this conjecture, the results of which will be reported in due course.

The behaviour of the dispersion relation in the vicinity of this wave front may be investigated for large Young's modulus by introducing the small non-dimensional parameter ε, defined by

$$\varepsilon = \frac{c}{c_5} \ll 1, \tag{6.1}$$

where c is a typical value of $c_j, j = 1, 2, 3, 4$. For the wave front an appropriate timescale is $O(c_5^{-1})$ and in view of this, and the satisfaction of boundary conditions,

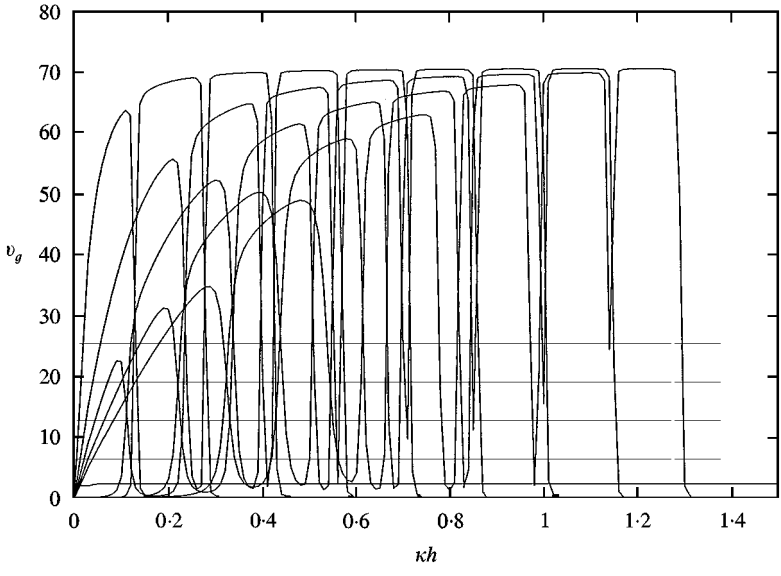

Figure 10. Group velocity curves showing v_g against kh, extensional waves, when $c_5^2 = 5000{\cdot}0$.

the following non-dimensional variables are introduced:

$$x_1 = h\xi, \qquad x_3 = h\varepsilon\zeta, \qquad t = \frac{h}{c_5}\tau. \tag{6.2}$$

The two appropriate equations of motion, equations (2.9) and (2.11) are now expressible in the form

$$c_5^2 \frac{\partial^2 u_1}{\partial \xi^2} + \varepsilon^{-2} c_3^2 \frac{\partial^2 u_1}{\partial \zeta^2} + \varepsilon^{-1}(c_3^2 + c_4^2)\frac{\partial^2 u_3}{\partial \xi \partial \zeta} - c_5^2 \frac{\partial^2 u_1}{\partial \tau^2} = 0, \tag{6.3}$$

$$\varepsilon^{-1}(c_3^2 + c_4^2)\frac{\partial^2 u_1}{\partial \xi \partial \zeta} + c_3^2 \frac{\partial^2 u_3}{\partial^2 \xi^2} + \varepsilon^{-2} c_1^2 \frac{\partial^2 u_3}{\partial \zeta^2} - c_5^2 \frac{\partial^2 u_3}{\partial \tau^2} = 0, \tag{6.4}$$

with the appropriate traction components given by

$$\sigma_{13} = \frac{\rho}{h} c_3^2 \left(\varepsilon^{-1}\frac{\partial u_1}{\partial \zeta} + \frac{\partial u_3}{\partial \xi}\right), \qquad \sigma_{33} = \frac{\rho}{h}\left(c_4^2 \frac{\partial u_1}{\partial \xi} + \varepsilon^{-1} c_1^2 \frac{\partial u_3}{\partial \zeta}\right). \tag{6.5}$$

From this longitudinal wave front it is expected that $u_1 \ll u_3$ and we therefore introduce non-dimensional displacement and traction components u_1^*, u_3^*, σ_{13}^* and σ_{33}^*, these being related to u_1, u_3, σ_{13} and σ_{33} through

$$u_1 = hu_1^*, \qquad u_3 = \varepsilon h u_3^*, \qquad \sigma_{13} = \varepsilon\rho c_5^2, \qquad \sigma_{33} = \varepsilon^2 \rho c_5^2 \sigma_{33}^*, \tag{6.6}$$

in which

$$\sigma_{13}^* = D_3\left(\frac{\partial u_1^*}{\partial \xi} + \varepsilon^2 \frac{\partial u_3^*}{\partial \zeta}\right), \qquad \sigma_{33}^* = D_4 \frac{\partial u_1^*}{\partial \xi} + D_1 \frac{\partial u_3^*}{\partial \zeta} \tag{6.7}$$

and the non-dimensional constants D_k are defined by $c^2 D_k^2 = c_k^2$. In terms of u_1^* and u_3^* the equations of motion (6.3) and (6.4) take the form

$$\frac{\partial^2 u_1^*}{\partial \xi^2} + D_3 \frac{\partial^2 u_1^*}{\partial \zeta^2} - \frac{\partial^2 u_1^*}{\partial \tau^2} + \varepsilon^2 (D_3 + D_4) \frac{\partial^2 u_3^*}{\partial \xi \partial \zeta} = 0, \tag{6.8}$$

$$(D_3 + D_4) \frac{\partial^2 u_1^*}{\partial \xi \partial \zeta} + D_1 \frac{\partial^2 u_3^*}{\partial \zeta^2} - \frac{\partial^2 u_3^*}{\partial \tau^2} + \varepsilon^2 D_3 \frac{\partial^2 u_3^*}{\partial \xi^2} = 0. \tag{6.9}$$

The relative orders of the displacement and stress components in terms of the original variables are given by

$$u_3 \sim \varepsilon u_1, \qquad \sigma_{13} \sim \varepsilon \sigma_{11}, \qquad \sigma_{33} \sim \varepsilon^2 \sigma_{11}. \tag{6.10}$$

The appropriate leading order solution for u_1 and u_3 are then given by

$$u_1 = \left(\sum_{m=1}^{2} \frac{-\mathrm{i}\eta(q_m)}{q_m} W^{(m)} \mathrm{e}^{k q_m x_3} \right) \mathrm{e}^{\mathrm{i}k(x_1 - vt)}, \qquad u_3 = \left(\sum_{m=1}^{4} W^{(m)} \mathrm{e}^{k q_m x_3} \right) \mathrm{e}^{\mathrm{i}k(x_1 - vt)} \tag{6.11}$$

in which

$$q_{1,2} = \pm \frac{\sqrt{c_5^2 - v^2}}{c_3}, \qquad q_{3,4} = \pm \frac{\mathrm{i}v}{c_1}. \tag{6.12}$$

A glance at equation (6.10) indicates that this leading order solution must be subject only to the boundary condition $\sigma_{13} = 0$ at $x_3 = \pm h$, leading to the approximate dispersion relations

$$v^2 = c_5^2 + \frac{(2n+1)^2 \pi^2}{4k^2 h^2} c_3^2, \quad v^2 = c_5^2 + \frac{n^2 \pi^2}{k^2 h^2} c_3^2 \tag{6.13}$$

for flexural and extensional waves respectively.

7. CONCLUDING REMARKS

In this paper high and low wave number expansions of the dispersion relations associated with flexural and extensional wave propagation in a fibre-reinforced plate have been derived. Although many excellent algorithms have been developed to solve dispersion relations numerically [18], the approximations derived in this paper offer a valuable and potentially highly useful alternative. In particular, it is envisaged that they will prove particularly useful in determining the dynamic stress response of a fibre-reinforced plate to impulsive events, especially in respect of high-velocity impact and internal impulsive events, such as delamination and cracking. For such problems the resulting transient response will involve a wide range of frequencies (and wavelengths), with stress variation through thickness changing rapidly. This is a situation quite distinct from that encountered in low-frequency vibration, or low-velocity impact, problems for which various

approximate techniques have proved extremely effective, offering methods capable of producing accurate results, [19, 20].

A specific and important physical problem for which a detailed knowledge of the stress variation is crucial is for prediction of material response arising from multiple high-velocity impact. For such problems the directional focussing of waves arising from an impact can cause weakening of the inter-ply bonds at locations away from the immediate impact site, these weakened regions being significantly more susceptible to delamination as a result of further impact [21]. In respect of high-velocity impacts, and internal impulsive events, methods based on the full three-dimensional equations have been specifically developed. One commonly used approach involves the use of integral transforms to obtain exact transform solutions for displacement and stress at any location within a plate or laminate. The dependence on space and time is then obtained by numerical inversion of these transform solutions. For line load problems the denominator of the integrand is the associated dispersion relation, each point on a branch therefore being a pole of the integrand. The inversion necessitates summing the integral contribution from each of its infinite number of branches over the infinite wave number range. Such integrals are highly oscillatory, especially for large wave number, and their convergence is often very slow.

The high wave number expansions derived in this paper offer an alternative representation of the dispersion relation which will not only save considerable computational time, but might well enable the numerical error associated with the aforementioned numerical inversions to be estimated. These errors arise because the numerical quadrature is truncated at some finite wave number and the summation is restricted to a finite number of harmonics. This is a method which is extremely attractive in view of the remarkable agreement between numerical, the numerical solution and approximations observed in Figures 7 and 8. Estimation of the effects of neglecting harmonics in the summation is of particular interest in respect of wave fronts arising from the cumulative effect of the harmonics, such as the longitudinal front discussed in this paper. For laminated media this is even more critical as surface and interfacial wave fronts can also be formed in this way [9, 11, 22]. In passing it is noted that in the third of these papers high wave number expansions for the phase speed are derived for an incompressible 4-ply (initially isotropic) laminated structure which is subject to an initial finite homogeneous pre-stress. In the case of multi-layered structures composed of layers of transversely isotropic elastic material, extension of the techniques discussed in the present paper will therefore be possible. Moreover, for general directions of in-plane propagation the cubic equation in q^2, analogous to equation (2.20), may be factorized [1], making the derivation of such expansion possible for propagation along any in-plane direction.

For numerical algorithms to determine dispersion relations, the efficiency of numerical schemes could be improved by using asymptotic approximation as an initial guess. Indeed, with the recent development of mathematical manipulation packages it is quite possible to develop a symbolic algorithm and call it directly from a numerical code. There then exists the potential for development of hybrid

asymptotic numerical routines using the methods developed in this paper as an algebraic algorithm.

A final point worth noting is that recently there have been examples of dispersion curves presented in the literature for which extensional and flexural harmonics exhibit oscillatory behaviour in the high wave number regime and continually cross over as the phase speed approaches the high wave number limit. This phenomena even occurs for a plane strain approximation and therefore is quite distinct from the well-known intersection with horizontally polarized shear waves [23, 24]. For non-symmetric laminated structures the implication is that numerical problems arise around these double roots. In such cases, the use of asymptotic methods to approximate the dispersion relation and help explicate its qualitative features is invaluable. In the context of the present paper, the oscillatory behaviour will occur when inequality (3.2) is violated. Investigation of this, more general directions of propagation and multi-layered media will form the basis of a future studies; the results of which will be reported in due course.

ACKNOWLEDGMENT

This work was supported by a grant awarded by the University of Salford Embryonic Research Committee. The authors are most grateful for this support.

REFERENCES

1. W. A. Green 1982 *Quarterly Journal of Mechanics and Applied Mathematics* **35**, 485–507. Bending waves in strongly anisotropic elastic plates.
2. P. Chadwick and V. S. Captain 1986 *Quarterly Journal of Mechanics and Applied Mathematics* **39**, 327–342. Surface waves in a transversely isotropic elastic body.
3. D. E. Chimenti 1997 *Applied Mechanics Reviews* **50**, 247–284. Guided waves in plates and their use in materials characterisation.
4. M. J. S. Lowe 1995 *IEEE Transactions on UFFC* **42**, 525–542. Matrix techniques for modeling ultrasonic waves in multilayered media.
5. L. P. Solie and B. A. Auld 1973 *Journal of Acoustical Society of America* **54**, 50–65. Elastic waves in free anisotropic plates.
6. L. Yan and R. B. Thompson 1990 *Journal of Acoustical Society of America* **87**, 1911–1931. Influence of anisotropy on dispersion characteristics of guided ultrasonic plate modes.
7. S. P. Pelts and J. L. Rose 1997 *Journal of Acoustical Society of America* **99**, 2124–2129. Source influence parameters on elastic guided waves in an orthotropic plate.
8. A. Mal 1988 *Wave Motion* **10**, 257–266. Wave propagation in layered composites under periodic surface loads.
9. G. A. Rogerson 1992 *Journal of Sound and Vibration* **158**, 105–120. Penetration of impact waves in a six-ply fibre composite laminate.
10. V. L. Beresin, L. Y. Kossovitch and J. D. Kaplunov 1995 *Journal of Sound and Vibration* **186**, 37–53. Synthesis of the dispersion curves for a cylindrical shell on the basis of approximate theories.
11. W. A. Green 1991 *Reviews of progress in QNDE* **10**, 1407–1414. Reflection and transmission phenomena of transient stress waves in fibre composite laminates.
12. A. J. M. Spencer 1972 *Deformations of Fibre-Reinforced Materials*. Clarendon Press: Oxford.

13. M. Musgrave 1970 *Crystal Acoustics*. Holden-Day: San Francisco.
14. P. Chadwick and A. M. Whitworth 1986 *Quarterly Journal of Mechanics and Applied Mathematics* **39**, 309–325. Exceptional waves in a constrained elastic body.
15. J. D. Kaplunov, L. Y. Kossovitch and E. V. Nolde 1998 *Dynamics of thin walled elastic bodies*. New York: Academic Press.
16. M. Markham 1970 *Composites* **1**, 145–149. Measurement of elastic constants of fibre composites by ultrasonics.
17. G. A. Rogerson and N. H. Scott 1992 *Acta Mechanica* **92**, 129–141. Aspects of energy propagation in highly anisotropic elastic solids.
18. B. Pavlakovic, M. Lowe, D. Alleyne and P. Cawley 1997 *Reviews of progress in QNDE* **16**, 185–192. Disperse: a general purpose program for creating dispersion curves.
19. C. T. J. Sun 1973 *Computational Mathematics* **7**, 366–382. Propagation of shock waves in anisotropic plates.
20. M. T. Wu and G. S. Springer 1988 *Journal of Computational Mathematics* **22**, 533–560. Impact induced stresses and delamination in composite plates.
21. S. Stone and A. K. Chatterjee 1990 *ASME-AMD* **116**, 27–50. Impact response and elastodynamics of composites.
22. G. A. Rogerson and K. J. Sandiford 1997 *Quarterly Journal of Mechanics and Applied Mathematics* **50**(4), 597–624. Flexural waves in pre-stressed incompressible elastic composites.
23. R. W. Ogden and D. G. Roxburgh 1993 *International Journal of Engineering Science* **30**, 1611–1639. The effect of pre-stress on the vibration and stability of elastic plates.
24. G. A. Rogerson 1998 *Journal of Mechanics and Physics of Solids* **46**(**9**), 1581–1612. On the existence of surface waves and the propagation of plate waves in pre-stresed, fibre-reinforced composites.